Interplanetary Mission Analysis and Design

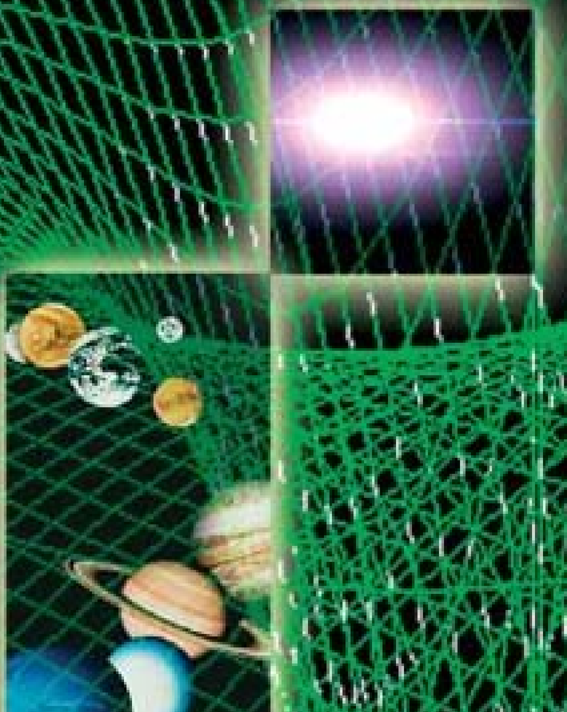

Stephen Kemble

With CD-ROM

Springer

PRAXIS

Interplanetary Mission Analysis and Design

Stephen Kemble

Interplanetary Mission Analysis and Design

Springer

Published in association with
Praxis Publishing
Chichester, UK

PRAXIS

Mr Stephen Kemble
Consultant
EADS Astrium
Stevenage
Hertfordshire
UK

SPRINGER–PRAXIS BOOKS IN ASTRONAUTICAL ENGINEERING
SUBJECT *ADVISORY EDITOR*: John Mason M.Sc., B.Sc., Ph.D.

ISBN 10: 3-540-29913-0 Springer-Verlag Berlin Heidelberg New York

Springer is part of Springer-Science + Business Media (springeronline.com)

Bibliographic information published by Die Deutsche Bibliothek

Die Deutsche Bibliothek lists this publication in the Deutsche Nationalbibliografie; detailed bibliographic data are available from the Internet at http://dnb.ddb.de

Library of Congress Control Number: 2005935455

Printed in Germany

Cover design: Jim Wilkie
Project copy editor: Bob Marriott
Project management: Originator Publishing Services, Gt Yarmouth, Norfolk, UK

Printed on acid-free paper

Contents

Preface ix

Acknowledgements xiii

List of figures xv

List of tables xxvii

Nomenclature xxxi

1 Interplanetary missions 1
- 1.1 Fundamentals of interplanetary missions 1
  - 1.1.1 Interplanetary transfers 1
  - 1.1.2 Lambert's problem 4
  - 1.1.3 Solutions to Lambert's problem for an interplanetary transfer 10
  - 1.1.4 Transfer types 16
  - 1.1.5 Launch opportunities 19
  - 1.1.6 Multi-revolution transfers 20
- 1.2 Leaving a planet 23
  - 1.2.1 Escape orbits 23
  - 1.2.2 Orbiting a planet 25
  - 1.2.3 Intermediate launch and apogee raising 25
  - 1.2.4 Interplanetary departure implications 38
- 1.3 Planet orbit selection and insertion 43
  - 1.3.1 Planetary approach and capture 43
  - 1.3.2 Target orbit options 43
- 1.4 Transfers through the Solar System 49
  - 1.4.1 Mercury 49
  - 1.4.2 Venus 49

1.4.3 Mars . . . 52
1.4.4 Jupiter . . . 53
1.4.5 Saturn . . . 55
1.4.6 Uranus, Neptune and Pluto . . . 56
1.5 Return missions to the planets . . . 58
1.5.1 Optimal stay times . . . 58
1.5.2 Case of an optimal stay time for a Mars return mission 61
1.5.3 Short-stay time missions at Mars . . . 63
1.5.4 Short-duration Mars return missions . . . 67

2 Spacecraft propulsion . . . 73
2.1 Propulsion basics . . . 74
2.2 High-thrust systems . . . 77
2.2.1 Chemical propulsion systems . . . 77
2.2.2 Thermal rockets . . . 78
2.3 Low-thrust systems . . . 79
2.3.1 Electric propulsion . . . 80
2.3.2 Solar sails . . . 84
2.4 Choice of propulsion system . . . 86

3 Optimisation . . . 89
3.1 The trajectory optimisation problem . . . 89
3.2 Trajectory optimisation methods . . . 91
3.2.1 Indirect optimisation techniques . . . 91
3.2.2 Direct optimisation techniques . . . 95
3.2.3 An example of control parameterisation . . . 95
3.2.4 Techniques for solving direct optimisation problems . . . 97
3.2.5 Selection of appropriate techniques . . . 106
3.3 Application of direct trajectory optimisation methods . . . 107
3.3.1 Formulating the mathematical problem . . . 107
3.3.2 Evaluation of gradients . . . 115
3.3.3 Non-linear programming . . . 124
3.4 Combining system and trajectory optimisations: the optimal transport problem . . . 127
3.4.1 Propulsion system optimisation parameters . . . 127

4 Special techniques . . . 135
4.1 Motion in multi-body gravity fields . . . 135
4.1.1 The multi-body problem . . . 135
4.1.2 Identifying the dominant gravity field . . . 137
4.1.3 Motion in the three body problem . . . 141
4.2 Escape from a planet . . . 145
4.2.1 Analysis of escape . . . 146
4.2.2 Examples of escape . . . 155
4.3 Principles of gravity-assist manoeuvres . . . 168

4.3.1 Analysis of patched conics 168
4.3.2 Plane-changing by gravity assist 184
4.3.3 Multiple gravity assists and resonance 194
4.3.4 Tisserand's criterion 201
4.3.5 Multiple gravity assists for plane-changing 206
4.3.6 Gravity assist at planetary moons for escape and capture 213
4.3.7 Modelling gravity assist manoeuvres 219
4.3.8 Anatomy of a gravity assist 222
4.4 The variational equations of Lagrange and Gauss 226
4.4.1 Orbital perturbations 226
4.4.2 Lagrange's planetary equations 226
4.4.3 Secular effects 230
4.5 Low-thrust transfers 233
4.5.1 Low-thrust transfer fundamentals 233
4.6 Low thrust for planetary escape and capture 245
4.6.1 Using thrust-coast arcs for energy gain 245
4.6.2 Application of a low-thrust strategy for escaping Earth . 247
4.6.3 Planetary capture and orbit insertion with low thrust . . . 253
4.6.4 Optimal utilisation of low-thrust for interplanetary transfers 253
4.7 Combining low thrust with gravity assist 257
4.7.1 Use of manoeuvres between gravity assists 257
4.7.2 The Earth gravity assist escape loop 257
4.7.3 Examples of raising aphelion with single Earth gravity assist 259
4.7.4 Examples of raising aphelion with double Earth gravity assist 268
4.8 Using multi-body gravity perturbations 272
4.8.1 The three-body problem 272
4.8.2 The Lagrange libration points 274
4.8.3 Orbits at the Lagrange libration points 282
4.8.4 Transfers to the Lagrange libration points 285
4.8.5 Gravity-assisted planetary escape and capture 298
4.8.6 Use of low thrust and gravitational escape 324
4.8.7 Summary of gravitational escape and capture techniques 325
4.9 Aerocapture and aerobraking 327
4.9.1 Aerocapture 327
4.9.2 Aerobraking 329

5 Missions to the planets 335
5.1 Interplanetary missions using gravity assist 335
5.1.1 Routes through the inner planets: mission to Mercury . . 335
5.1.2 Messenger to Mercury 352
5.1.3 Gravity assist for Mars return missions 355
5.1.4 Reaching Jupiter 356

5.1.5 Gravity-assisted tours of Jupiter's moons 362
5.1.6 Transfers to the outer planets 368
5.1.7 Missions to minor bodies 379
5.1.8 Escaping the Solar System 382
5.2 Low-thrust missions 389
5.2.1 Analysis of a low-thrust, multi-gravity assist mission to Mercury 389
5.2.2 Analysis of missions to Jupiter and Saturn using low thrust 397
5.2.3 Missions to Pluto with low-thrust 407
5.3 Missions using gravity escape and capture 409
5.3.1 Transfer from Jupiter to Saturn 410
5.3.2 Transfer from Jupiter to Uranus 417
5.3.3 Analysis of a mission to Venus using capture via the Lagrange points 421

Appendix 1: Keplerian orbits 429

Appendix 2: Frames of reference 443

Appendix 3: The planets 449

Appendix 4: Optimising launcher injection 459

Index 477

Preface

One of the enduring legacies of the twentieth century will be the advent of space travel. This achievement has changed the way we think about our presence in the Universe and now offers the possibility to explore beyond our own world. Nobody experiencing the Apollo missions of the 1960s and 70s could be unaffected by the magnitude of those achievements. Now, nearly forty years later, space travel is almost commonplace, although man's personal presence in space is still limited.

The pioneering edge of space exploration now lies beyond Earth and its moon, as numerous spacecraft over the last thirty years have visited most of the planets of the Solar System. Mars remains the focus of many such missions and is likely to be the first planet that man visits personally, not just through robotic craft. Perhaps the most fascinating interplanetary missions to date have been the Voyagers. Launched in the late 1970s, these spacecraft were flung out of the Solar System after flying by the outer planets. They have now passed far beyond Pluto as they leave the Sun's domain behind.

These technical achievements have inspired numerous science fiction stories, which in turn have themselves perhaps influenced the drive for new space missions and exploration. Although 'warp drives' remain for the present in the realm of science fiction, more adventurous missions to explore our Solar System are being planned. These include an initiative to place a man on Mars and also for a detailed robotic exploration of Jupiter and its family of moons. This later system has already been inspected by the Galileo spacecraft and revealed a fascinating 'micro solar system' with a rich variety of features. Also, both current (Messenger) and planned future missions (Bepi–Colombo) to Mercury will undertake the difficult route to the innermost planet of the Solar System. In addition to the planets, the minor bodies of the Solar System are being explored. A challenging example is ESA's Rosetta mission, following a complex route to achieve a rendez-vous with a comet.

MISSION ANALYSIS AND DESIGN

This diverse range of missions require numerous techniques for their analysis and design. These aspects will be considered in this book, including the key issues of escaping from a planet, interplanetary transfer, and capture at a target planet. Certain 'classical' methods for the design of such trajectories have been employed for many years. As missions became more demanding, then new techniques were developed to enable more efficient designs to be realised. These allow the efficient utilisation of newly evolving propulsion technologies. This theme is continuing, as both new mathematical and computational ideas are considered for the solution of these problems.

The objective of this book is to describe a selection of techniques that may be applied to the analysis and design of interplanetary missions. The focus is on methods that enable the efficient solution of the problems considered. Details of the methods are given. However, this text is not intended as a reference on astrodynamics. Summaries of key derivations are included.

The terms 'mission analysis' and 'mission design' can have several meanings. The one taken here is that of the analysis and design of spacecraft transfers. Therefore, the focus is on techniques in orbital mechanics and trajectory optimisation that may be applied to the objective. The aspects of mission analysis particularly relevant to interplanetary missions are considered here.

This book is divided into five major chapters. The first chapter focuses on 'conventional' analysis and design techniques for interplanetary missions. This includes the basic ideas of Hohmann transfers, the solution of Lambert's problem and the fundamentals of planetary escape and capture. These basic ideas of interplanetary transfers are then extended to consider return missions to the planets. The issue of escape from Earth is also considered in more detail, in the context of the efficient utilisation of launch vehicle capabilities. This subject is also further expanded in Appendix 4.

The second chapter briefly considers aspects of spacecraft propulsion systems. These systems are a fundamental factor in the nature of interplanetary mission designs and therefore warrant some consideration in a book such as this.

The third chapter focuses on optimisation. In particular, methods for obtaining solutions to local optimisation problems are considered. These generally require gradient evaluations and are often called 'gradient based' methods. These methods are essential for the efficient design of interplanetary missions. As more complex propulsion system types are considered, so the complexity of the optimisation problems increases. Many developments are taking place in this area. Only gradient-based methods are considered here. However, it should be noted that alternative techniques such as evolutionary computing offer very interesting prospects for the identification of globally optimal solutions. In addition to trajectory optimisation problems, the nature of spacecraft optimisation is discussed, where the design of the propulsion installation may be optimised together with the transfer trajectory.

The fourth chapter considers a range of 'special' methods that may be employed for mission analysis and design. These methods allow the planning of more efficient transfers. A consequence of the improved efficiency is the increased complexity of the transfer routes. Some of these methods take advantage of interesting features of astrodynamics. A good example of this is the phenomenon of gravitational escape or capture at a planet, which has been observed for comets in the Solar System. Consequently, this chapter contains an outline description of the three-body problem and mission designs that can utilise three-body effects. Many of the techniques considered in this chapter allow the efficient utilisation of advanced propulsion system concepts. This is particularly true for low-thrust systems. The effect of low thrust systems on orbit evolution is considered via the application of perturbation equations. Considerable attention is paid to 'gravity assist'. This technique allows the utilisation of combined gravity fields to enable a spacecraft to significantly modify its orbital energy, without the need for manoeuvre.

The final chapter describes a series of mission examples that utilise the methods described in the previous sections. These include missions using gravity assist, low-thrust propulsion, gravitational escape and capture. Many of the examples are generic, in that they consider typical transfers between planets. However, certain examples are relevant to actual missions, either past, current, or future.

The appendices describe the basics of orbital mechanics, orbital reference frames, and also the properties of the planets. The data is intended as a source of reference for the material in the book.

A CD is included to give some examples of interplanetary missions. A simulation tool is included. This is used to generate animated sequences that show interplanetary transfers. The missions illustrated include both transfers to the inner and outer planets. Instructions for use are contained on the CD. The software runs on Windows based PC systems.

Although every effort has been made to eliminate mathematical and factual errors in the material in this book, complete accuracy cannot be guaranteed. Please send any errors found and suggested corrections to the author.

Acknowledgements

I would like to thank numerous groups and individuals. First, project teams within the European Space Agency (ESA), with whom I have worked. This work has provided much of the background for the material in this text, particularly through the diverse series of projects undertaken. Specifically, the Bepi–Colombo project led by J. Van Casteran with lead mission analyst R. Jehn, the Science Payloads and Advanced Concepts, planetary exploration studies team led by P. Falkner, the Lisa–Pathfinder project led by G.Racca with lead mission analyst M. Landgraf, the SOLO project led by N. Rando with lead mission analyst G. Janin and also M. Hechler, J. Rodriguez Canabal, and W. Flury on a wide range of projects. I would like to thank the many colleagues at EADS Astrium with whom I work, particularly those with whom I regularly work (or have worked) directly on mission analysis topics, including C. Warren, M.J. Taylor, A. Povoleri, and G. Hughes.

I would also like to specifically thank R.C. Parkinson, for support and always asking the most interesting questions!

Also many thanks to Clive Horwood at Praxis and Neil Shuttlewood at Originator.

Figures

1.1.1 Planetary orbital energy with respect to the Sun relative to Earth's energy with respect to the Sun . . . 3
1.1.2 Hohmann transfer between circular planetary orbits. . . . 3
1.1.3 Lambert's problem . . . 5
1.1.4 Error function versus sma . . . 8
1.1.5 Lambert's problem for a transfer between two planetary orbits . . . 9
1.1.6 The velocity change required when departing the first planet. . . . 10
1.1.7 Transfer V_∞ contours for a transfer from an idealised circular Earth orbit to an idealised Mars circular orbit at zero inclinations . . . 11
1.1.8 Transfer V_∞ contours for a transfer from Earth orbit to an idealised Mars orbit possessing zero inclination, but with normal eccentricity . . . 12
1.1.9 Transfer V_∞ contours for a transfer from Earth to Mars . . . 13
1.1.10 Total Vinfinity versus transfer duration for a launch on 23 October 2011. . . . 14
1.1.11 Transfers from Earth to Mars for a launch on 23 October 2011, for a range of transfer durations spanning the two minima and the central maximum in V_∞ 15
1.1.12 Transfer types between planets . . . 16
1.1.13 Optimum transfer between planets and accelerated and delayed arrival . . . 17
1.1.14 2011 transfers from Earth to Mars . . . 18
1.1.15 A set of transfers occurring with a given synodic period and making up a global repeat period after three synodic repeat periods . . . 20
1.1.16 A 1.5-revolution transfer for a launch in 2011 . . . 21
1.1.17 Extended-duration transfers in terms of Vinfinity contours, for Earth–Mars transfers starting 2011 . . . 22
1.2.1 Departure orbit geometry. . . . 24
1.2.2 Apogee altitude vs pericentre ΔV to reach a given Vinfinity with perigee altitude at 200 km . . . 26
1.2.3 Apogee altitude vs pericentre ΔV to reach a given Vinfinity with perigee altitude at 2000 km . . . 26
1.2.4 ΔV required to reach required excess hyperbolic speed for conjunction-class transfers from Earth . . . 27

1.2.5 Orbital energy per unit mass of a 100,000-km semi-major-axis orbit with respect to the planet escape condition 27
1.2.6 Fuel tank limited performance for spacecraft injection to high apogee and elliptical orbits 31
1.2.7 Fuel tank limited performance for spacecraft injection to high apogee and hyperbolic orbits 32
1.2.8 Mass components versus intermediate injection apogee radius 34
1.2.9 A case of fixed upper stage mass showing spacecraft mass versus intermediate injection apogee radius, for a target apogee of 1.5 million km for two spacecraft propulsion mass fractions. 34
1.2.10 A case of fixed upper stage mass showing spacecraft useful mass versus intermediate injection apogee radius, for a range of target escape orbit Vinfinity, and for a spacecraft propulsion mass fraction of 0.15. 35
1.2.11 A second case of fixed upper stage mass showing spacecraft useful mass versus intermediate injection apogee radius, for a range of target escape orbit Vinfinity, for a spacecraft propulsion mass fraction of 0.15 36
1.2.12 ΔV from injection orbit to 1.5-million km apogee target orbit. 36
1.2.13 Example of apogee raising from a 42,000 km apogee injection orbit to reach a target orbit with apogee of 1.5 million km. 37
1.2.14 ΔV from injection orbit to 5 km/sec excess speed 38
1.2.15 The departing hyperbolic orbit, showing the asymptotic true anomaly 39
1.2.16 The departure vector seen within the orbit plane of the escape hyperbola, showing two alternative solutions attaining the same departure direction 40
1.2.17 Simulation of two hyperbolic orbits with ascending nodes separated by 180 degrees (inclinations 60 and 120 degrees) achieving a 30 degree asymptotic departure declination 41
1.2.18 The effect of declination requirement on the hyperbolic orbit argument of perigee for a 3 km/sec excess hyperbolic speed orbit leaving Earth 42
1.3.1 Definition of the B plane 44
1.3.2 The relationship between Beta angle and inclination, for a range of different declinations. 45
1.3.3 Arrival geometry seen in the orbit plane about the planet 46
1.3.4 The effect of excess hyperbolic speed between 3,000 and 5,000 m/s on possible pericentre locations for approaches to Mars and Venus at zero declination . . 47
1.3.5 The effect of approach declination between 0° and 30° on possible pericentre locations for approaches to Mars with an excess hyperbolic speed of 3 km/sec 48
1.3.6 A hyperbolic approach to Venus with a pericentre retro-burn to reach a 5-day transfer orbit about Venus 48
1.4.1 V_∞ sums for conjunction type two-impulse transfers to Mercury over the launch period 2007 50
1.4.2 V_∞ sums for conjunction type 2 impulse transfers to Venus over the launch period 2010–2013 52
1.4.3 V_∞ sums for conjunction type, two-impulse transfers to Jupiter over launch period 2009. 54
1.4.4 Vinfinity sums for conjunction-type two-impulse transfers to Saturn over launch period 2009–2010 57
1.5.1 Return mission geometry 59
1.5.2 The effect of stay time on V_∞ total for different conjunction-type transfers for launch in 2011 to Mars 62

1.5.3 The effect of stay time on V_∞ total for different transfer types for launch in 2020 64
1.5.4 Transfer options from Mars to Earth leaving in 2021, with two local minima in V_∞ totals . . . 65
1.5.5 A return mission to Mars with optimal conjunction-type transfer (launch in 2020) on the outward leg, 60-day stay-time, and minimum ΔV trajectory on the return leg . . . 66
1.5.6 The effect of stay-time on return ΔV and V_∞ after a short conjunction-class transfer from Earth, departing in mid-2020 . . . 68
1.5.7 The effect of stay time on total mission duration after a short conjunction-class transfer from Earth, departing in mid-2020 . . . 69
1.5.8 A fast return transfer from Mars to Earth with a short stay at Mars after a conjunction-class outward transfer . . . 69
1.5.9 Examples of short transfers from Earth to Mars with short stay-time and return 70

2.1.1 Illustration of a nozzle . . . 76
2.3.1 A gridded ion thruster in operation. . . . 81
2.3.2 A conceptual illustration of a Hall-effect thruster . . . 82
2.3.3 The principle of the solar sail . . . 84
2.3.4 A solar sail concept proposed by NASA . . . 86

3.2.1 An example of a parameterisation of a continuously variable steering angle . . 96
3.2.2 Trajectory segmentation used by multiple shooting algorithms . . . 98
3.2.3 Initial trajectory segmentation for multiple shooting, for the case of a transfer from Earth escape orbit to Jupiter approach using two Earth GAs . . . 99
3.4.1 Thrust arc dependence on thrust/mass for an apogee raising manoeuvre of 100 km . . . 132
3.4.2 The relationship between ΔV loss and thrust for a low-thrust apocentre raise manoeuvre of 100 km. . . . 132
3.4.3 The relationship between fuel mass, specific impulse and thrust for a low-thrust apocentre raise manoeuvre of 100 km with an initial mass of 1,000 kg . . . 133

4.1.1 Illustration of gravitational equality 'sphere' . . . 138
4.1.2 Motion in the presence of two gravity fields . . . 139
4.1.3 Orbital geometry in the circular, restricted three-body problem . . . 145
4.2.1 Relative velocity geometry . . . 148
4.2.2 Idealised planetary escape geometry by vector addition of an instantaneous excess hyperbolic departure vector . . . 149
4.2.3 Motion relative to the planet after departure . . . 150
4.2.4 Transfer from Earth to raised aphelion orbit with Earth Vinfinity at 2.3 km/sec 156
4.2.5 Semi-major axis and energy with respect to Earth, evolution over distance from circular orbiting Earth . . . 157
4.2.6 Osculating excess hyperbolic speed evolution with respect to Earth, evolution over distance from circular orbiting Earth . . . 157
4.2.7 Energy with respect to Sun, evolution over distance from a circular orbiting Earth . . . 158
4.2.8 Angular momentum with respect to Sun, evolution over distance from circular orbiting Earth . . . 159

4.2.9 Semi-major axis and energy with respect to Earth, evolution over distance from circular orbiting Earth, for a radial Earth relative departure case 160
4.2.10 Transfer from Earth to increased eccentricity orbit with Earth relative radial Vinfinity at 2.3 km/sec 161
4.2.11 Energy with respect to Sun, evolution over distance from circular orbiting Earth, for a radial Earth departing case 161
4.2.12 Comparison of Earth relative semi-major axis evolution for two-body and three-body departure cases 162
4.2.13 Comparison of Earth relative range evolution for two-body and three-body departure cases 163
4.2.14 Comparison of Earth relative angular momentum evolution for two-body and three-body departure cases 164
4.2.15 Transfer from Jupiter to reduced perihelion orbit with Jupiter osculating Vinfinity at 5.86 km/sec 164
4.2.16 Semi-major axis with respect to Jupiter, evolution over distance from Jupiter . 166
4.2.17 Excess hyperbolic speed with respect to Jupiter, evolution over distance from Jupiter 166
4.2.18 Semi-major axis and energy with respect to Sun, evolution over distance from Jupiter 167
4.3.1 The principle of patched conics 170
4.3.2 Deflection of the asymptote velocity vector 172
4.3.3 Geometry of the 2D fly-by with coplanar planet and spacecraft orbits 172
4.3.4 Alternative deflection possibilities for 2D fly-by 173
4.3.5 Velocity vector addition at the fly-by for a 2D case 173
4.3.6 Two possible locations for a fly-by 175
4.3.7 The rotation of the line of apses after a gravity assist at location 1 176
4.3.8 The rotation of the line of apses after a gravity assist at location 2 176
4.3.9 The effect of fly-by altitude on the final orbit 177
4.3.10 The effect of initial orbit perihelion and eccentricity on gravity assist effectiveness at Venus 178
4.3.11 The effect of initial orbit excess hyperbolic speed on gravity assist effectiveness at Venus for different initial aphelions 179
4.3.12 The effect of initial orbit perihelion and eccentricity on gravity assist effectiveness at Earth 180
4.3.13 The effect of gravity assists at different Jovian moons for the same spacecraft orbits 182
4.3.14 The effect of gravity assists on orbital energy at different Jovian moons for the same spacecraft orbits 183
4.3.15 Velocity vector addition at the ΔV assisted fly-by 184
4.3.16 The effectiveness of ΔV at pericentre of Jupiter fly-by 185
4.3.17 Definition of the B plane and approach plane 187
4.3.18 The fly-by plane and the relationship between Beta angle, deflection angle, deflection angle components and the approach plane 188
4.3.19 Definition of deflection angles and axis set 189
4.3.20 Definition of relationships between the initial approach plane and major body orbit plane 191
4.3.21 Post-Ganymede gravity-assist Jupiter-centred speed versus fly-by Beta angle, evaluated for a range of approach orbit pericentres from 500,000 to 900,000 km 194
4.3.22 Post-Ganymede gravity-assist Jupiter-centred inclination, apocentre and

pericentre change, versus fly-by Beta angle, evaluated for a range of approach orbit pericentres from 500,000 to 900,000 km 195
4.3.23 Post-Ganymede gravity-assist Jupiter-centred inclination and apocentre change, polar plot versus fly-by Beta angle, evaluated for a range of approach orbit pericentres from 600,000 to 900,000 km 196
4.3.24 Post-Ganymede gravity-assist Jupiter-centred inclination and apocentre change loci, evaluated for a range of approach orbit pericentres, between 700,000 and 900,000 km 197
4.3.25 Relative velocity in a resonant orbit 197
4.3.26 Limiting fly-by geometry 198
4.3.27 Apocentre and pericentre evolution for a Ganymede gravity assist sequence in the Jovian system 199
4.3.28 Examples for four resonant gravity assists at Ganymede. 200
4.3.29 Orbital period–pericentre relationship for gravity assist at Earth for a range of excess hyperbolic speeds between 3,000 and 5,000 m/s. 203
4.3.30 Apocentre–pericentre relationship for gravity assist at Earth for a range of excess hyperbolic speeds between 3,000 and 5,000 m/s. 203
4.3.31 Apocentre–pericentre relationship for gravity assist at Venus for a range of excess hyperbolic speeds from 3,000 to 7,000 m/s 204
4.3.32 Apocentre–pericentre relationship for gravity assists at Earth and Venus for a range of excess hyperbolic speeds. Speeds of 3,000 to 5,000 m/s at Earth are considered, and 3,000 to 7,000 m/s at Venus 205
4.3.33 Apocentre–pericentre relationship for gravity assist at Europa, Ganymede and Callisto for a range of excess hyperbolic speeds 205
4.3.34 Period–pericentre relationship for gravity assist at Europa, Ganymede and Callisto for a range of excess hyperbolic speeds 206
4.3.35 The definition of deflection angles in a multi-gravity assist case 207
4.3.36 Two gravity assists maintaining resonance, showing both approach planes . . . 209
4.3.37 Effect of progressive deflection of the fly-by plane for resonant orbits targeted at inclination increase 210
4.3.38 Limiting case defining maximum inclination relative to the major body orbit plane when in a resonant orbit 211
4.3.39 A maximum inclination case when central body relative velocity may be varied at subsequent fly-bys from V_1 to V_{limit} 212
4.3.40 Example of multiple resonant gravity assists at Ganymede, with excess hyperbolic speed at Ganymede of 9.5 km/sec 212
4.3.41 Inclination, aphelion and perihelion evolution for a sequence of gravity assist at Venus with Vinfinity at 22.4 km/sec. 214
4.3.42 Orbit evolution for a sequence of gravity assist at Venus 215
4.3.43 The effect of apogee altitude on Earth excess hyperbolic speed after lunar fly-by for a fly-by altitude of 260 km 216
4.3.44 The effect of ΔV for apogee raising on Earth excess hyperbolic speed 216
4.3.45 The principle of planetary capture using gravity assist at a moon 217
4.3.46 Approach excess hyperbolic speed versus target Jupiter pericentre altitude after Ganymede fly-by for a range of post-gravity assisted captured apocentre altitudes 218
4.3.47 Approach excess hyperbolic speed versus target Saturn pericentre altitude after Tital fly-by for a range of post-gravity assist captured apocentre altitudes . . . 218

4.3.48 Gravity assisted transfer at Earth to reach raised aphelion with Earth V_∞ at 6 km/sec . . . 223
4.3.49 Semi-major axis and energy with respect to Earth during an Earth gravity assist, evolution over distance from Earth . . . 223
4.3.50 Excess hyperbolic speed with respect to Earth during an Earth gravity assist, evolution over distance from Earth . . . 224
4.3.51 Semi-major axis with respect to Sun during an Earth gravity assist, evolution over distance from Earth . . . 224
4.3.52 Energy with respect to Sun, evolution over distance from Earth . . . 225
4.5.1 Evolution of a near circular orbit with constant perturbing acceleration perpendicular to the radius vector . . . 235
4.5.2 A comparison of optimum and zero steering-angle options for increasing the semi-major axis for an initial elliptical orbit with an eccentricity of 0.73 (GTO) 237
4.5.3 A low-thrust trajectory with maximum rate of change of semi-major axis steering over a period of nearly 9 days . . . 237
4.5.4 Low-thrust semi-major axis evolution with maximum rate of change of semi-major axis and zero α steering over a period of nearly 9 days . . . 238
4.5.5 A comparison of optimum and zero steering-angle options for increasing the semi-major axis for an initial elliptical orbit with an eccentricity of 0.37. . . . 238
4.5.6 A comparison of optimum apogee raising and optimum semi-major axis raising steering-angle options for increasing apogee for an initial elliptical orbit with an eccentricity of 0.73 (GTO) . . . 239
4.5.7 A comparison of steering angles for optimum apogee raising and optimum semi-major axis raising steering-angle options for increasing apogee for an initial elliptical orbit with an eccentricity of 0.73 (GTO) . . . 240
4.5.8 A low-thrust trajectory with maximum rate of change apogee altitude steering over a period of nearly 9 days . . . 240
4.5.9 A comparison of optimum apogee raising and optimum semi-major axis raising steering angle options for increasing apogee for an initial elliptical orbit with an eccentricity of 0.37 . . . 241
4.5.10 Low-thrust GTO trajectory evolution with thrust/mass at 0.0004 and initial inclination at 1° . . . 242
4.5.11 Low-thrust GTO trajectory evolution with thrust/mass at 0.0004 and initial inclination at 1° . . . 243
4.5.12 Low-thrust heliocentric 1-AU orbit ephemeris evolution with thrust/mass at 0.0004 m/s/s and initial inclination at 1° . . . 243
4.5.13 Low-thrust heliocentric 1-AU trajectory evolution with thrust/mass at 0.0004 m/s/s and initial inclination at 1°, over a period of two years . . . 244
4.6.1 The change in semi-major axis per unit applied ΔV versus true anomaly . . . 245
4.6.2 The change in semi-major axis per unit applied ΔV (time averaged over an applied true anomaly range) versus true anomaly range from perigee. . . . 246
4.6.3 The change in semi-major axis per unit applied ΔV (time averaged over an applied true anomaly range) versus true anomaly range from perigee. . . . 246
4.6.4 Transfer duration and ΔV dependence on initial circular orbit altitude in reaching Earth escape . . . 248
4.6.5 Transfer from GTO to earth escape . . . 249
4.6.6 Transfer from GTO to Earth escape with 60-degree coast phase at apogee . . . 250
4.6.7 The effects of coast arcs on ΔV and the time to escape for the transfer to Earth escape using lunar gravity assist and direct thrust to Earth escape . . . 251

4.6.8 ΔV versus thrust and transfer duration for low-thrust Earth escape from GTO 252
4.6.9 ΔV needed to reach a given Vinfinity from an initial GTO orbit about Earth. 254
4.6.10 The effect of Earth departure V_∞ on total transfer fuel usage for a Mars approach V_∞ of 500 m/s 256
4.6.11 The effect of Mars approach V_∞ on total transfer fuel usage for an Earth departure V_∞ of 1,000 m/s 256
4.7.1 Example of a scheme for utilisation of Earth gravity assist 258
4.7.2 ΔV implications to reach alternative targets by varying initial orbit aphelion, the initial V_∞ is 1,500 m/s and inwards departure is used 260
4.7.3 $\Delta V/V_\infty$ change ratio implications to reach alternative targets by varying the initial orbit aphelion 261
4.7.4 ΔV implications to reach alternative targets by varying initial orbit aphelion . 261
4.7.5 Thrust-mass of 0.2 and 0.1 N/t for transfer to a 2.2-AU orbit 263
4.7.6 The ΔV penalty for reducing thrust/mass for transfer to a 2.2-AU target 264
4.7.7 Comparison of observed and predicted ΔVs for reaching target aphelion or equivalently targetting Earth relative V_∞ 264
4.7.8 Comparison of observed ΔV using final manoeuvre after EGA and predicted ΔVs for reaching target aphelion or equivalently targetting Earth-relative V_∞ 265
4.7.9 Comparison of ΔVs for reaching target aphelion for a two-burn strategy (pre EGA) and the effect of introducing a third burn after Earth gravity assist . . . 265
4.7.10 Transfer to a 2.87-AU orbit using strategy B 266
4.7.11 The effect of a final post-EGA burn for case B 267
4.7.12 Transfer to a 2.87-AU orbit using strategy C 267
4.7.13 The effect of a final, post-EGA burn for case C 268
4.7.14 Comparison of ΔVs and EGA Vinfinities for the three alternative cases over a range of target aphelions 269
4.7.15 Effect of manoeuvre on achievable excess hyperbolic speed at Earth and post-GA aphelion in a 2-year Earth resonant orbit 270
4.7.16 The use of a double EGA to raise aphelion to a target at 10 AU, using manoeuvres in the two-year resonant loop and also after the final EGA. 271
4.7.17 The use of a double EGA to raise aphelion to a target at 80 AU, using manoeuvres in the two-year resonant loop and also after the final EGA. 271
4.7.18 The deep-space ΔV required to reach a target aphelion after a low-energy escape after lunar gravity assist and 2 EGAs 272
4.8.1 Zero-velocity boundaries for the Earth–Sun system, showing the zone centred on Earth on the rotating system X axis 274
4.8.2 Zero-velocity boundaries for the Jupiter–Sun system, showing a wide area zone centred on the Jupiter and Sun co-linear Lagrange points 275
4.8.3 The positions relative to the two bodies in the rotating reference frame 276
4.8.4 Locations of the Lagrange libration points 277
4.8.5 A manifold at the Earth–Sun L1 Lagrange point exhibiting Lissajous and high Earth elliptical orbit behaviour 287
4.8.6 Energy and angular momentum variation over a manifold at the Earth–Sun L1 Lagrange point exhibiting Lissajous and initial high Earth elliptical orbit behaviours 288
4.8.7 Manifolds at the Earth–Sun L1 Lagrange point exhibiting Lissajous and initial high Earth elliptical orbit behaviours, for a range of initial orbit osculating semi-major axes from 575,000 to 700,000 km 289

4.8.8 Energy and angular momentum variation over manifolds at the Earth–Sun L1 Lagrange point exhibiting Lissajous and initial high Earth elliptical orbit behaviours, for a range of initial orbit osculating semi-major axes between 575,000 and 700,000 km 290
4.8.9 Manifolds at the Earth–Sun L1 Lagrange point exhibiting Lissajous and initial high Earth elliptical orbit behaviours, for a range of initial orbit osculating perigee altitudes from 500 to 36,000 km 292
4.8.10 Energy and angular momentum variation over manifolds at the Earth–Sun L1 Lagrange point exhibiting Lissajous and initial high Earth elliptical orbit behaviours, for a range of initial orbit osculating perigee altitudes from 500 to 36,000 km 293
4.8.11 State transition elements showing final position sensitivity to initial velocity, for a manifold linking low Earth perigee to a Lissajous orbit at L1 295
4.8.12 Transfer evolution starting from near Earth perigee with variations in argument of perigee of 0.05° 296
4.8.13 Transfer evolution of a 775000 semi-major axis initial orbit starting from near-Earth perigee, with variations in right ascension of ascending node of an approximately 110 degrees, reaching free injection Lissajous orbits 296
4.8.14 Transfers from a 500 km perigee orbit to Lissajous orbits about the Earth–Sun L1 point, showing transfers both north and south of the ecliptic 299
4.8.15 Transfers from a 500-km perigee orbit to Lissajous orbits about the Earth–Sun L1 point, showing transfers both north and south of the ecliptic and motion in the rotating *YZ* plane 300
4.8.16 Variation in rotating frame relative velocity with *X* and *Y* displacement in the Earth–Sun system for Jacobi: constant at the reference value 302
4.8.17 Variation in rotating frame relative velocity with *X* and *Y* displacement in the Earth–Sun system for the case of the incremented Jacobi constant 303
4.8.18 Planet relative velocity 304
4.8.19 Variation in Earth relative energy (using rotating frame radial velocity vector direction assumption and reference Jacobi constant value) with rotating frame *X* and *Y* displacement 304
4.8.20 Variation in Earth relative energy using radial (top) and prograde (middle) and retrograde (bottom) rotating frame velocity vector directions, with *X* and *Y* rotating frame displacement and reference Jacobi constant value 306
4.8.21 Escape from an initial Earth-bound orbit with a semi-major axis of 1.8 million km, using gravitational assistance 312
4.8.22 Evolution of Earth relative semi-major axis and energy from initial bound orbit to escape 313
4.8.23 Evolution of angular momentum and position–velocity angle from the initial bound orbit to escape 314
4.8.24 Evolution of Sun-relative semi-major axis and angular momentum from initial Earth bound orbit to escape 316
4.8.25 Escape from lower energy initial Earth bound orbit and evolution of Sun-relative semi-major axis 317
4.8.26 Transfer to a large-amplitude free injection Lissajous orbit from initial orbit with a semi-major axis of 1.8 million km 318
4.8.27 Evolution of energy and semi-major axis with distance from Earth, for a transfer to a large amplitude free injection Lissajous orbit 319

4.8.28 Evolution of Sun relative semi-major axis and angular momentum from initial perigee to free injection orbit 320
4.8.29 Escape from an initial Jupiter-bound orbit with semi-major axis of 25 million km, using gravitational assistance 321
4.8.30 Evolution of Jupiter relative semi-major axis and energy from initial bound orbit to escape 322
4.8.31 Evolution of Sun relative semi-major axis and angular momentum from initial Jupiter bound orbit to escape 323
4.8.32 Using low-thrust apogee-raising for gravitational escape from initial GTO . . . 324
4.8.33 Gravitational escape after low-thrust apogee-raising 325
4.9.1 The principle of aerocapture. 329
4.9.2 Aerobraking drag and altitude profile during a typical pericentre passage. . . . 331
4.9.3 Aerobraking velocity and altitude profile over a period of 100 days 331
4.9.4 Aerobraking velocity and altitude profile over a period of 100–140 days 332
4.9.5 Aerobraking at Mars from a 100,000-km apocentre insertion orbit over a 100-day period 333

5.1.1 Transfer to Mercury in 2004: leaving Earth for Venus 346
5.1.2 Transfer to Mercury in 2004: Venus to Venus 4 : 3 resonant orbit 346
5.1.3 Transfer to Mercury in 2004: Venus to Mercury rendezvous after 1.5 revolutions 347
5.1.4 Transfer to Mercury in 2004: Venus to Mercury and Mercury 2 : 3 and 3 : 4 resonant orbits 347
5.1.5 Transfer to Mercury in 2012: motion relative to Mercury during the last two 1 : 1 resonant orbits 348
5.1.6 Transfer with VGA/VGA/MGA/MGA/MGA/MGA/MGA for 2004 case . . . 350
5.1.7 Transfer with VGA/VGA/MGA/MGA/MGA/MGA/MGA for 2004 case, showing out-of-ecliptic motion 350
5.1.8 Transfer with VGA/VGA/MGA/MGA for 2009 launch case. 351
5.1.9 Messenger type mission: initial Earth to Venus and Venus 1 : 1 resonant phases 353
5.1.10 Messenger type mission 354
5.1.11 Messenger type mission. Transfer with VGA/VGA/MGA/MGA/MGA for final Earth departure in August 2005, showing motion out of the ecliptic 354
5.1.12 Return from Mars via Venus gravity assist 356
5.1.13 The V-V-E Cassini mission launched in 1989 and adapted to terminate at Jupiter 359
5.1.14 The V-E-E Galileo mission, launched in 1989 360
5.1.15 Multiple gravity assist transfer with a launch in 2012 361
5.1.16 Period–pericentre loci for a range of Ganymede and Europa Vinfinities 363
5.1.17 Gravity assist and manoeuvre sequence in the Jovian system for orbit insertion strategy 1 at Europa plotted over period–pericentre loci at Ganymede and Europa. 365
5.1.18 Gravity assist and manoeuvre sequence in the Jovian system for orbit insertion strategy 2 at Europa plotted over period–pericentre loci at Ganymede and Europa. 366
5.1.19 Sequence of gravity assists at Ganymede and Europa 367
5.1.20 Minimum ΔV transfer to Neptune with a V-E-E-J sequence after launch in 2013 370
5.1.21 Minimum ΔV transfer to Neptune with a V-E-E-J sequence after launch in 2013 but with an upper limit on transfer duration 371